International Journal of Applied Earth Observation and Geoinformation 15 (2012) 38–48

Contents lists available at ScienceDirect

International Journal of Applied Earth Observation and Geoinformation

journal homepage: www.elsevier.com/locate/jag

Monitoring urban changes based on scale-space filtering and object-oriented classification

G. Doxani [a,*], K. Karantzalos [b], M. Tsakiri- Strati [a]

[a] *Aristotle University of Thessaloniki, Dept. Cadastre, Photogrammetry and Cartography, 54124 Thessaloniki, Greece*
[b] *Remote Sensing Laboratory, National Technical University of Athens, 15780 Athens, Greece*

ARTICLE INFO

Article history:
Received 30 September 2010
Accepted 18 July 2011

Keywords:
Object-based image analysis
Multivariate alteration detection
Morphological scale space filtering

ABSTRACT

This paper introduces a multi-temporal image processing framework towards an efficient and (semi-) automated detection of urban changes. Nonlinear scale space filtering was embedded in an object-based classification procedure and the resulted simplified images provided a more compact and reliable source in order to generate image objects in various scales. In this manner the multiresolution segmentation outcome was constrained qualitatively. Multivariate alteration detection (MAD) transformation was applied afterwards on the simplified data to facilitate the detection of possible changes. The altered image regions along with the simplified data were further analyzed through a multilevel knowledge-based classification scheme. The developed algorithm was implemented on a number of multi-temporal data acquired by different remote sensing sensors. The qualitative and quantitative evaluation of change detection results performed with the help of the appropriate ancillary ground truth data. Experimental results demonstrated the effectiveness of the developed scale-space, object-oriented classification framework.

1. Introduction

The automatic and accurate recognition of land cover changes in urban environment, through the integrated analysis of multi-temporal remote sensing data, is of fundamental importance towards the efficient updating of geographic information systems, government decision-making, urban land management and planning. Although urban land cover changes can be monitored by traditional ground survey and photogrammetric procedures, nowadays high resolution satellite remote sensing sensors provide a cost-effective source of information for detecting important spatial patterns of land cover change over a large geographic area in a recurrent way. To this end, there is plenty of research nowadays towards exploiting the geo-information of multi-temporal remotely sensed data (Hall and Hay, 2003; Baltsavias, 2004; Bergen et al., 2005; Im and Jensen, 2005)

In particular numerous research efforts have studied extensively the problem of detecting changes in multi-temporal data. Lu et al. (2004) studied the most popular pre- and post-classification methods for various applications and grouped them into seven types of change detection methods: algebra, transformation, classification, advanced models, geographical information system (GIS) approaches, visual analysis and some other approaches. Another recent review by Sui et al. (2008) categorized the change detection techniques in seven categories: namely, direct comparison, classification, object-oriented methods, model method, time series analysis, visual analysis and the hybrid method. Despite the differences regarding the categorization approach (Li et al., 2003; Radke et al., 2005), it has been generally accepted that there is not any specific single methodology that is appropriate for all applications and/or all case studies (Sui et al., 2008).

Besides, the development of automated approaches designed for the accurate monitoring of urban land cover changes remains a major research issue. Photo-interpretation, traditional ground survey and manual digitization of land cover changes may deliver an accurate product but they are time-consuming and inappropriate to record the rapid alterations of urban areas (Steinnocher and Kressler, 2006; Champion et al., 2010). To this end, the automation of change detection process for the efficient updating of geospatial databases has gained significant attention lately (Holland et al., 2008; Bouziani et al., 2010).

Advanced methods are likely to have a model-based structure and to take into consideration the available intrinsic information of the objects such as colour, texture, shape and size, and topological information as location and neighborhood (Blaschke, 2004; Lang, 2008; Champion et al., 2009). A recent three-step approach was proposed by Ouma et al. (2008) in order to exploit the textural and spectral image information. Firstly, the wavelet transformation was employed for decomposing images into the details and the overall pattern. Then a multispectral anisotropic diffusion was applied and the resulted smoothed images were classified in an

* Corresponding author. Tel.: +30 2310996146; fax: +30 2310996128.
E-mail addresses: gdoxani@topo.auth.gr (G. Doxani), karank@central.ntua.gr (K. Karantzalos), martsaki@topo.auth.gr (M.T. Strati).

0303-2434/$ – see front matter © 2011 Elsevier B.V. All rights reserved.
doi:10.1016/j.jag.2011.07.002

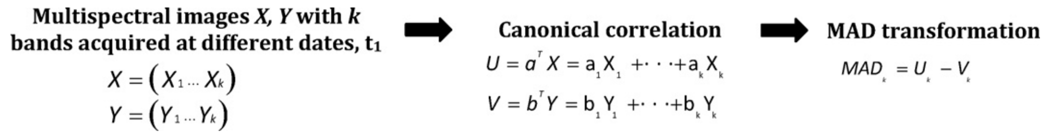

Fig. 1. The basic implementation steps of multivariate alteration detection (MAD) transformation.

unsupervised manner from a self-organizing neural network. A logical-operations-based model was finally applied for the detection of the changed areas.

Other studies are also employing available ancillary data, usually vector information, along with imagery data in order to facilitate the process. Bouziani et al. (2010), for example, utilized nicely the vector layers from an existing geodatabase regarding the position of urban objects (buildings, roads, etc.). They created then a relevant knowledge-based and defined proper change detection rules for associating image objects and prior information. In a similar way, Champion et al. (2010) used the existing vector information from an available database in combination with images and digital surface models (DSM). A mask containing the above-ground objects was extracted from the DSM and then a classification into certain classes (buildings, trees, etc.) was realized based on the multispectral image information. The extraction of new buildings was accomplished through the comparison of the resulted buildings to the existing geodatabase.

Despite recent research efforts the automatic and accurate urban change detection from multi-spectral/temporal data remains a challenge (Baltsavias, 2004; Champion et al., 2009; Matikainen et al., 2010). The latest satellite sensors may provide imagery of higher spatial and spectral resolution, but still the different light, atmospheric and soil moisture conditions at the different dates of imagery acquisition, the complexity of urban environment and the spectral, shape and size variation of man-made objects hinder the automation of accurate change detection (Donnay et al., 2001; Jensen, 2005; Champion et al., 2009; Bouziani et al., 2010). The aforementioned variables limit the effectiveness of traditional change detection approaches-like image algebra, image transformation techniques or post-classification analysis. Thus, novel and more sophisticated algorithms are required (Holland et al., 2008) that are also efficient in cases where only single optical images (the most cost-effective data nowadays) are available. On the one hand, there are cases where vector or height information (DSM) is not available or cases where the acquisition of stereo pairs (e.g. Worldview II) costs approximately twice as much as a single image acquisition.

In addition, several important aspects of earth observation data cannot be analyzed based on pixel information, but they can only exploited based on the contextual information and the topologic relations of the objects of interest through a multiscale image analysis (Blaschke, 2010; Tzotsos et al., in press). Starting with the observed spatial heterogeneity and variability, meaningful spatial aggregations (objects) can be formed at certain image scales configuring a relationship between image objects and real-world objects. With such an object-based multiscale analysis including certain hierarchically structured rules, the relationship between the different scales of the spatial entities can be defined (Baatz and Schape, 2000; Benz et al., 2004; Hay and Castilla, 2006; Aplin and Smith, 2008; Zhou et al., 2009; Blaschke, 2010; Tzotsos et al., in press).

To this end, in this paper an advanced object-based classification framework is introduced towards the accurate and (semi-) automated monitoring of changes in the urban environment. Scale-space image analysis was employed providing compact image representations towards the generation of image objects in various scales i.e. object hierarchy. The multivariate alteration detection (MAD) algorithm (Nielsen, 1994; Nielsen et al., 1998) was computed on the simplified images for the detection of altered image pixels. Object-based image analysis was subsequently introduced for the efficient handling of changes by implementing a knowledge-based classification scheme. The developed algorithm was designed to provide a solution even when only optical satellite imagery (like WorldView II, GeoEye, Ikonos, Quickbird, etc.) is available, contrary to recent efforts where LIDAR or data from vector databases was utilized (Champion et al., 2010; Bouziani et al., 2010). Another contribution of the paper is that advanced scale space filtering, MAD transform and object-based image analysis have been efficiently embedded in a single knowledge-based processing framework (Fig. 1) for the analysis of multi-temporal imagery.

The paper is structured in the following way. The proposed change detection methodology based on pixel-based pre-processing, included scale-space filtering and MAD transformation, as well as object-oriented classification is described in Section 2. The applications on the imagery data and their results are analyzed in Section 3. The performed quantitative and qualitative evaluation of the developed methodology is presented in Section 4. Section 5 is dedicated to conclusions and future work.

2. Developed methodology

The developed change detection methodology is incorporating certain advanced image processing techniques, namely the non-linear scale space filtering, the multivariate alteration detection algorithm and a knowledge-based classification scheme through object-based image analysis. Filtering processes were employed towards generating more smooth representations of the original images. When working directly on the raw data one has to tackle the noise and the undesired detail in a certain spatial scale. Therefore, advanced scale space filtering is a common procedure in order to provide data that are more adequate for information extraction. In such a way the information of very high spatial resolution imagery data was easier to be handled in the following processing steps. Hence the segmentation result was ameliorated as more compact and homogeneous objects were produced. Moreover the change analysis of urban study area required auxiliary information concerning the altered areas. The implementation of multivariate alteration detection algorithm pointed out these image regions and facilitated the classification procedure.

2.1. Morphological scale space filtering

Morphological levelings are a powerful class of self-dual morphological filters, which recently have been proposed as an effective tool for image scale space simplification and segmentation (Meyer and Maragos, 2000; Meyer, 2004; Karantzalos et al., 2007).

Considering that a light region (Resp. dark region) is marked by a regional maximum (Resp. a regional minimum), one should look for connected operators which do not create any new extremum and which do not exchange a maximum of a minimum (and conversely). Being able to compare the values of “neighboring pixels” one can define levelings as a subclass of connected operators that preserve the grey-level order. Levelings are transformations $\Lambda(f, g)$ and in mathematical terms, based on a lattice framework, an image g is a leveling of the image f if and only if for all neighboring points in space (all neighbor pixels $\forall(p, q)$) the following equation holds:

$$g_p > g_q \Rightarrow f_p > g_p \text{ and } g_q \geq f_q \quad (1)$$

Levelings are created when they are associated to an arbitrary family of marker functions. These multiscale markers can be obtained from sampling a Gaussian scale-space. Let there be an original image $f(p, q)$ and a leveling Λ. Assuming that one can produce markers $h_i(p, q)$, $i = 1,2,3\ldots$, associated with an increasing scale parameter i and calculate the leveling $\Lambda(h_i, f)$ of image f based on these markers, a multiscale representation can be produced.

The implemented scale space representation is employing anisotropic diffusion filtering (ADF) defined by a geometry-driven diffusion (Alvarez et al., 1992; Karantzalos et al., 2007). The markers which control the leveling computation have been already smoothed through an anisotropic manner. To this end, resulted levelings were dominated by enhanced and smoothed images in which edges, abrupt intensity changes or other details have been respected. With such a reference image the multiscale markers obtained from sampling its Gaussian scale-space, did not start blurring the original image but they started from blurring the anisotropic diffusion filtering output.

2.2. Multivariate alteration detection (MAD)

The multivariate alteration detection change detection approach which was firstly proposed by Nielsen (1994) is, generally, an orthogonal transformation based on canonical correlation analysis between two groups of variables towards the calculation of the possible linear combinations that give the maximum multivariate differences. We assume that these groups of variables are two multispectral images, with k number of bands, which depict the same area and they were acquired at different dates, t_1 and t_2. If the images are represented at a given pixel by random vectors $X = [X_1 \ldots X_k]^T$ and $Y = [Y_1 \ldots Y_k]^T$, which are assumed to be multivariate normally distributed ($E\{X\} = E\{Y\} = 0$), then the simple difference D between the images is defined as $D = a^T X - b^T Y$. The a^T and b^T are a set of coefficients, in order to describe in a more flexible way the linear combinations of X and Y: $a^T X = a_1 X_1 + \ldots + a_k X_k$ and $b^T Y = b_1 Y_1 + \ldots + b_k Y_k$. To define the transformation coefficients vectors a^T and b^T, we maximize the Var $\{a^T X - b^T Y\}$, subject to the restriction that Var $\{a^T X\}$ = Var $\{b^T Y\} = 1$. In that way, the determination of difference between two linear combinations with maximum variance corresponds to linear combinations with minimum correlation (positive). In general the transformation coefficients vectors a^T and b^T are defined by a standard canonical correlation analysis. Briefly, the vectors a^T and b^T can be defined using the generalized eigenvalue problem. If k is the number of bands, the transformation calculates k eigenvalues, k pairs of eigenvectors and k uncorrelated MAD components. MAD components are calculated from the difference of the corresponding canonical variates (Fig. 1).

2.3. Decision thresholds for MAD components

To exploit the change information of the MAD components, it is required to distinguish the change from no-change pixels. The MAD variates follow approximately the normal distribution and tend to cluster around zero; they are also uncorrelated with each other, so the decision thresholds could be determined through standard deviation σ (Canty, 2007). The threshold value is set separately for each MAD component by considering that the intensity values that are within $\pm 2\sigma$ of zero are corresponding to no-change pixels. In the same way like in Canty (2007) the decision thresholds were defined automatically. The methodology is based on the consideration that a MAD component can be represented by a simple Gaussian mixture model for a random variable M. The probability density function of M can be formed by combining normal density components of the classes no change (NC), positive change (C+) and negative change (C−):

$$p(m) = p(m|NC)p(NC) + p(m|C-)p(C-) + p(m|C+)p(C+)$$

The expectation maximization (EM) algorithm is then used to calculate the parameters of the mixture model. The EM algorithm assigns posterior probabilities to each component density with respect to each observation. The upper and the lower threshold for each component can be determined as soon as the model parameters converge.

2.4. Object-based classification

The MAD transformation is an efficient way to indicate the possible changes, but similarly with other statistical algorithms, it cannot provide an automated solution for change detection. A classification process is required (Canty, 2007; Niemeyer et al., 2007; Nussbaum and Menz, 2008) to properly distinguish and label the type of the detected changes. Towards this end a dual object-based classification process was designed, developed and implemented in this study. The first one was responsible for delivering a ‘rough’ mask of the possible changed areas by employing MAD components. More specifically, two classes of changes were defined for each MAD component: one class for the positive changes (MAD+) and another for the negative ones (MAD−). Automatic thresholds calculated by EM algorithm facilitated the accurate definition of these classes. Identifying the possible altered regions ameliorated significantly the overall procedure, since the inappropriate areas (no-changed pixels) were eliminated and only the areas of interest (changed pixels) were further analyzed. To this end, the following knowledge-based classifier was responsible for a task of significant importance: moving from primitive (almost knowledge-free) image objects to semantic image objects, i.e. type of changes.

Therefore a knowledge-based classification was implemented along with the appropriate rule set for the efficient and accurate association of image objects with the exact type of change (class). The visual interpretation of MAD components and multispectral images assisted the association of image objects with the corresponding changes of land cover types. The possible alterations were related with changes in vegetation, bare soil and man-made objects (building, roads, etc.). In particular, regarding the building class it was not possible to treat all the buildings as a single class. Thus, different types and description of classes, including features, functions and thresholds, were defined for the design of the classification scheme. Various segmentation levels were created through the process of multiresolution segmentation towards facilitating the handling of each type of land cover change.

2.5. The overall knowledge-based change detection framework

A flowchart that describes the overall developed change detection methodology is presented in Fig. 2. Firstly, the raw data were simplified through a morphological scale space filtering. Then, the MAD transformation was applied on the smoothed data and the MAD components were calculated from the difference of the corresponding canonical variates. The automatic thresholding of MAD components indicated, in a generic manner, the changed image regions. In the next step of the algorithm and along with the simplified images from the scale space filtering, the individual MAD components were integrated into the object-based image analysis framework.

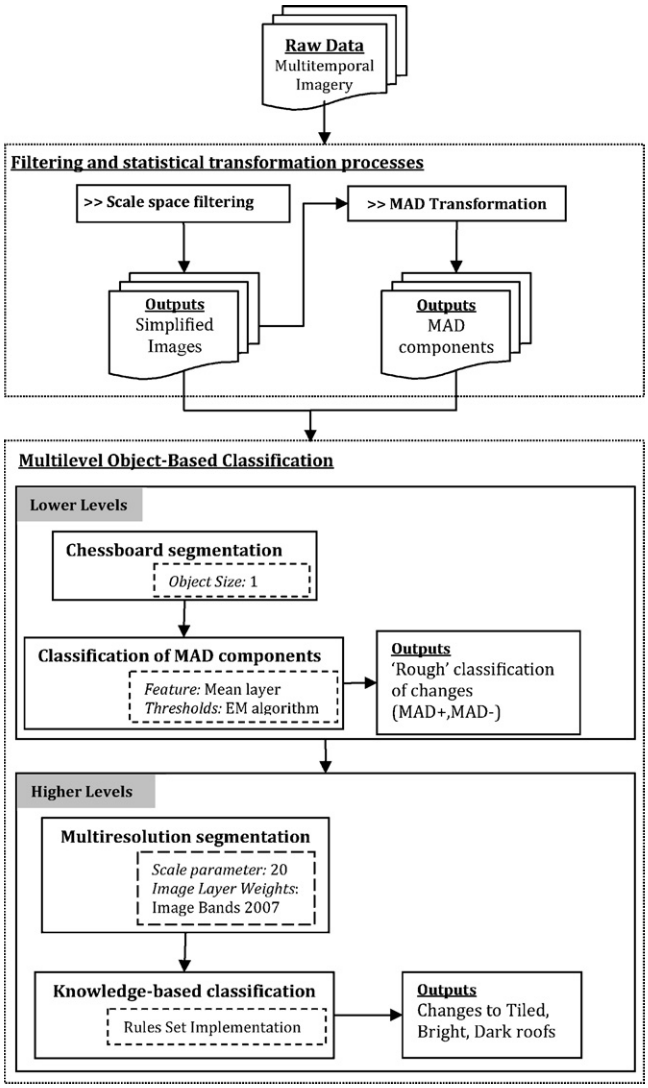

Fig. 2. The flowchart of the developed change detection methodology.

3. Experimental results and evaluation

3.1. Data pre-processing and ground truth

The developed methodology was applied to an available dataset of high resolution satellite images from five (5) different temporal acquisitions. In particular, the dataset included three (3) pan-sharpened Quickbird orthoimages, with spatial resolution of 0.6 m and radiometric resolution 16 bit, acquired in 2003, 2007 and 2008 and two (2) pan-sharpened Ikonos orthoimages, with spatial resolution of 1 m and radiometric resolution 16 bit, acquired in 2000 and 2006. All images depict the same part of city of Thessaloniki, in the North of Greece, specifically an urban area of Pilea suburb. The co-registration of the data was accomplished using as a reference the Quickbird image of 2007 and by applying a first order polynomial transformation and a nearest-neighbor resampling. Approximately a total of fifteen (15) ground control points were selected and the overall root mean square error (RMSE) was around 0.45 pixels for each image registration procedure. The radiometric (e.g. atmospheric) correction was not necessary since both the selected scale space simplification as well as the MAD transformation is robust and invariant regarding linear changes of the pixel intensities (Canty, 2007).

The quantitative and qualitative evaluation was performed with the help of the appropriate ancillary ground truth data. The ground truth information which included approximately 80 buildings derived after an extensive photo-interpretation and a manual digitization performed by an expert. The quantitative evaluation was performed by employing the standard performance evaluation measures of detection completeness, correctness and overall quality, which have been widely applied on building identification studies (Jin and Davis, 2005; Champion et al., 2010; Karantzalos and Paragios, 2009; Ozdemir et al., 2010). Both pixel-based and object-based criteria were used to evaluate the detection performance. Regarding the pixel-based evaluation we compared the detection result pixel-by-pixel with the ground truth, while in object-based evaluation we compared the detection result object-by-object. In both evaluation procedures we computed the standard performance evaluation measures of detection completeness, correctness and overall quality.

3.2. Evaluating the scale space filtering, the MAD transformation and the multi-resolution segmentation

Multitemporal imagery data were smoothed and simplified by morphological scale space filtering at different scales without losing important information like the edges of image objects (Fig. 3). Scale refers to the number of filtering iterations and thus, represents increasingly different levels of smoothness. As the simplification preserved image edges, the smoothing result was clearer in those regions without important alternations in intensity values (e.g. vegetation, buildings roofs, etc.). In the case that roofs were homogeneous, image edges corresponded to edges of objects of interest (roof-edges). On the contrary in the cases of roofs with windows, antennas or other information, the delineation of building edges was a more complicated task. After an extensive trial and error investigation the scale space filtering was applied with an upper limit for the coarser scale (i.e. smoothing scale parameter 1000). This kind of simplified data formed, qualitatively, a significantly enhanced input to the following MAD transformation and classification procedures. They describe image intensity with a more compact manner and by avoiding the interference of noise, pseudo-edges or other details.

The computed MAD components (MAD2, MAD3, MAD4) are illustrated in Fig. 4. The first MAD component was a noise image because it carried the maximum amount of change information; so it was excluded from the study data. The thresholds were derived automatically from the EM algorithm towards indicating the significant changes. The detected altered areas were marked by dark (MAD−) and bright (MAD+) pixel values. Areas with no changes were specified with grey pixel values. In this manner a mask of changed and no-changed pixels was defined. A visual interpretation of MAD images led to primary conclusions for the correspondence between pixel values and type of changes. Similar pixel values of MAD images represented similar type of change. In MAD3 for instance the transitions to tiled roofs (dark pixels) and to bright roofs (bright pixels) were highlighted (Fig. 4). Towards the semantic definition of change information, a further processing of MAD images took place through the object-oriented classification scheme.

A qualitative evaluation of the developed algorithm performance is presented in Figs. 5 and 6, regarding the scale space filtering and the multi-resolution segmentation. The experimental results, with and without the application of the scale space filtering, were compared, holding the segmentation scale parameter constant. In Figs. 5 and 6 one can clearly observe a significant difference in the shape as well the size of the resulted objects (segments). The borders of the buildings in the simplified images were more clearly delineated. Therefore, there was an actual association between the

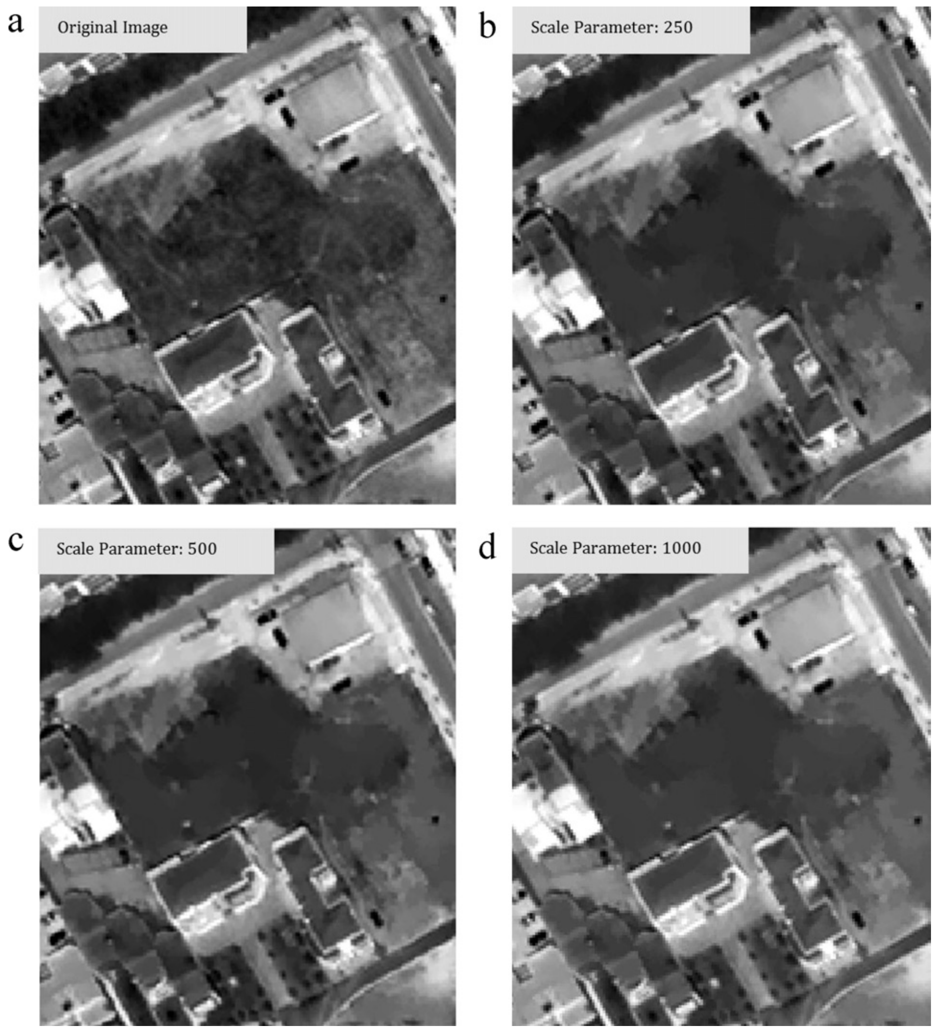

Fig. 3. Subsets of the Blue band of the reference image and the resulted simplified images at different smoothing scale parameters.

resulting objects and real-world features. It is worth mentioning that the generation of meaningful image objects is considered to be the main problem of segmentation especially in urban areas (Lizarazo and Barros, 2010; Smith and Morton, 2010). The developed algorithm, by embedding nonlinear scale space images into the multi-resolution segmentation, ameliorated the constructed object hierarchy qualitatively. This kind of filtering preserved image edges and improved the following processing steps by addressing the usual over/under-segmentation and misclassification problems (Karantzalos et al., 2007). What was also remarkable was the number of resulting objects in the two case studies. The number of the segmented objects after the scale space filtering was approximately the 1/5 of the initial objects, a fact that facilitated their handling and processing.

3.3. *Evaluating the multilevel object-based classification procedure*

For brevity's sake, the following developed rule set is referring to building change detection. The rule set was designed in a way to classify efficiently all the type of terrain features like building to those with (a) tiled roofs, (b) bright roofs and (c) dark roofs, based on their basic intensity level. To this end, the first classification process (Fig. 2) was introduced for delivering a 'rough' map of the detected changes depending mainly on MAD components. The chessboard segmentation with object size equal to a pixel was chosen, in order to define automatically the thresholds of classification rules, as they had been already calculated by EM algorithm (pixel-based process). Hence, the possible altered image regions were extracted and marked over the lower levels of the computed object hierarchy. This 'rough' mask played an important role in the following knowledge-based classification by providing a stable and reliable starting point for the association of object statistical attributes with the corresponding classes.

The subsequent classification rule set (Fig. 2) was created for the detailed analysis of the probable areas of changes, namely the determination of the exact type of alteration. Thus an efficient design of the knowledge-based presupposed to consider also the initial state of each type of terrain class. A part of the implemented rules set, utilizing the images of 2003 and 2007, is presented in Table 1 and is analyzed below. The transitions, for example, to tiled roofs were delineated by the following fuzzy rules (DTR, detection of tiled roofs):

- DTR1: If the Relative Area of sub objects MAD3− was high (greater than 0.45), then it was possibly a new structure with tiled roof. To confirm that these objects were actually buildings, the following rules were set to this object domain.
- DTR2: If the value of mean red 2007 was high (greater than 135) and mean blue 2007 was low (lower than 120), then the possibility for an object to be a new building with tiled roof was even higher.

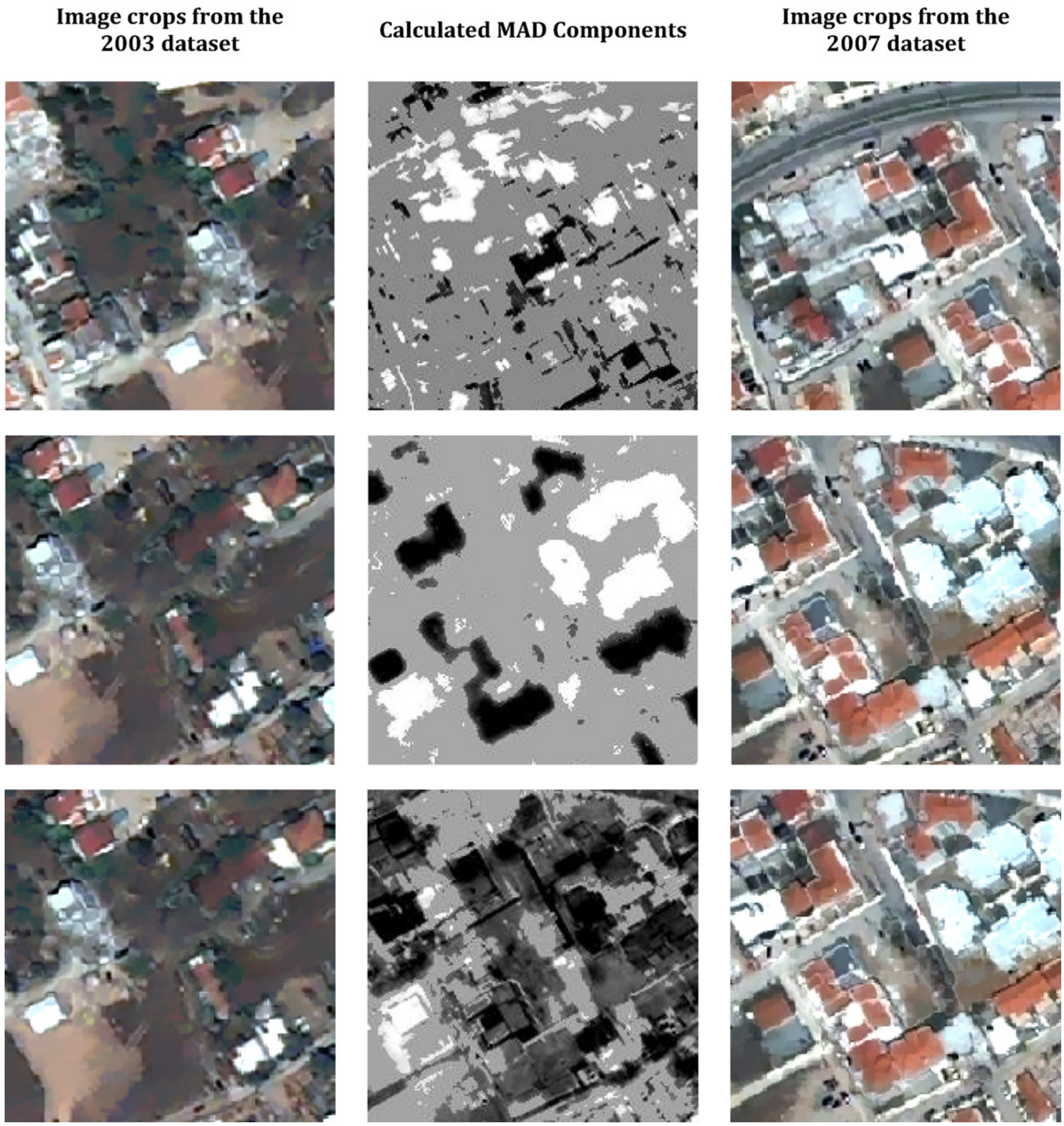

Fig. 4. The MAD Components as resulted after the application of the EM algorithm: MAD2 (top), MAD3 (middle), MAD4 (bottom). The detected changed were indicated by the dark (MAD−) and the bright (MAD+) pixel values. Areas with no detected changes were marked with grey pixel values.

- DTR2a: If the value of mean red 2003 of this object was also high (greater than 120) and the value of NDVI 2003 was low (lower than 0.4), then this object was a possible building with tiled roof in image of 2003, so it was incorrectly detected as change and excluded from further process.
- DTR2b: If the value of mean blue 2003 of an object was high (greater than 150) and the value of mean MAD4 was within a certain threshold (ranges from 180 to 220), then this object was possibly a building under construction in image of 2003 that resulted to a building with tiled roof in 2007.
- DTR3: If the value of shape features rectangular fit was low (lower than 0.7) and length/width was high (greater than 3), then this object was incorrectly detected as an altered building.

Briefly, the objective of the described rule set structure was to define initially the changes to tiled roofs based on the computed MAD component (DTR1). The resulted classified objects were separated into building with tiled roof and other changed image objects (DTR2). The following analysis was based on the spectral attributes of image objects of 2003 and improved the change detection result (DTR2a, DTR2b). Last but not least, the resulted misclassified objects (possibly shadows, occlusions, different soil moisture conditions, etc.) were excluded from any further process (DTR3) because of their inappropriate shape.

An additional rule set example addressed to the detection of bright roofs and it was defined following the proposed approach that described above. The change detection rules in this case were based mainly on the information of MAD3 component. A visual interpretation indicated that the possible alterations occurred from vegetation or bare soil to bright roofs (DBRs refers to detection of bright roofs rule set):

- DBR1: If the relative area of sub objects MAD3+ was high (greater than 0.45), then the object was possibly a new structure with bright roof.

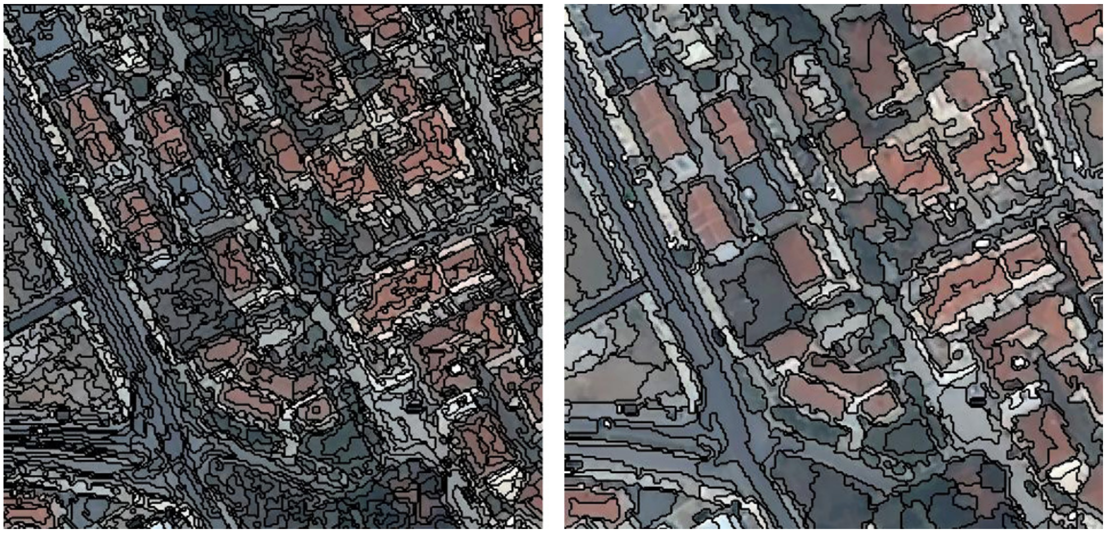

Fig. 5. The scale space filtering ameliorated the multi-resolution segmentation step. Left: results of segmentation at scale 20 when processing the original data delivered numerous image objects (11.351), impeding the following classification step. Right: the same segmentation scale but after processing the simplified images results to a significant lower and more manageable number (2.254) of image objects.

- DBR2: If the value of Brightness was high (greater than 140), then the possibility for an object to be a new building with bright roof was even higher.
- DBR2a: If the value of mean blue 2003 was high (greater than 135), then this object was possibly a building in image of 2003 and it was incorrectly detected as change.
- DBR3: If the value of shape features rectangular fit was low (lower than 0.7) and length/width was high (greater than 3), then this object was incorrectly detected as an altered building.

In an attempt to standardize the procedure and implement the already analyzed rules for defining the possible transitions to dark roofs, the main difficulty was the similar spectral signatures of buildings with the other man-made features. Particularly, regions of bare soil or vegetation in 2003 were basically changed to either buildings or roads in 2007. Consequently, these changes were calculated with very similar intensities values in MAD components, hindering their segregation. To this end, firstly all the possible alterations were detected (buildings, roads, parking lots, etc.) and then only the actual transitions to dark roofs were preserved through a gradual process. The main features of this rule set were the mean values of MAD2, MAD4, NDVI 2007 and the value of ratio blue 2007.

In order to assess the efficiency of the rule set and towards its standardization, we did several experiments by calculating the MAD components on the raw and the simplified data. The overall design and structure of the final developed rule set for both cases was similar. A part of the rules set defined for the classification of the raw data is presented in Table 2. The detected changes were initially classified as they were indicated in MAD components and then the classification result was refined. The features and the membership functions of the "simplified" fuzzy rule set were slightly altered in this implementation, but in general they

Fig. 6. The simplified images after the scale space filtering, by ameliorating the multi-segmentation step, facilitated the classifier to find more accurately the correct correspondences between image objects and terrain classes. Building from the ground truth data overlaid to the computed segments when processing the original (left) and the simplified (right) data.

Table 1
Part of the developed Rules Set regarding the classification of the simplified images.

Domain	Class name	Features	Membership function	Threshold value	Purpose
Unclassified	Changes to tiled roofs	Relative area of sub objects MAD3−	Larger than	0.4–0.45	To classify new buildings with tiled roofs as indicated in MAD3
Changes to tiled roofs	Real tiled roofs	Mean red 2007/mean blue 2007	Larger than/smaller than	130–135/120–130	To identify the changes with high possibilities to be building with tiled roof
Real tiled roofs	Unclassified	Rectangular fit/length/width	Smaller than/larger than	0.7–0.8/2.5–3	To identify the rectangular objects that were definitely buildings
Unclassified	Changes to bright roofs	Relative area of sub objects MAD3+	Larger than	0.4–0.45	To classify new buildings with bright roofs as indicated in MAD3
Changes to bright roofs	Real bright roofs	Brightness	Larger than	130–140	To identify the changes with high possibilities to be building with bright roof
Real bright roofs	Unclassified	Rectangular fit/length/width	Smaller than/larger than	0.7–0.8/2.5–3	To identify the rectangular objects that were definitely buildings
Unclassified	Changes to dark roofs	Mean MAD4	About range	50–150	To classify new buildings with dark roofs as indicated in MAD4
Changes to dark roofs	Real dark roofs	Mean MAD2/ratio blue 2007	Larger than/larger than	200–210/1.5–1.6	To identify the changes with high possibilities to be building with dark roof
Real dark roofs	Unclassified	Rectangular fit/length/width	Smaller than/larger than	0.7–0.8/2.5–3	To identify the rectangular objects that were definitely buildings

coincided with the description of DTRs, DBRs, etc. Nevertheless, the tuning of the thresholds, in the case of raw dataset was necessary due to different intensity values and significant dissimilarities in the shape and size of resulted segments. However the definitions of “low” and “high” values facilitated the determination of the corresponding thresholds. To this end, the most considerable differentiation between the two rule sets was the integration of additional rules regarding the shape optimization of the classified objects. A loop process of region growing algorithm was initially used to refine their shape. Shape properties like area, compactness, etc. were then utilized to optimize the shape of detected objects and remove image noise (mainly misclassified objects or relatively small objects without any semantic information).

Experimental results from the application of the multi-level knowledge-based classification are presented in Figs. 7–9. Although, results do not seem to differentiate significantly after a close inspection one can observe otherwise. In the first case (developed multilevel knowledge-based classification) all the detected changes regarding entire entities (single objects) were correct without any false alarm in contrast to the case where the MAD components were computed directly from the raw data. The shape of the majority of classified objects was more compact in the first case. The homogenized image regions facilitated the creation of terrain objects (building) with a shape that fitted better to their actual/correct one. Therefore, during the classification process the spectral overlap between the different urban land cover features was addressed to some extent by the developed algorithm and the resulted classified objects were generally more compact, discrete and well bounded.

4. Results and discussion

A quantitative evaluation based both on pixel-based and object-based criteria was performed, in order to confirm the aforementioned qualitative observations (Table 3). The standard measures of detection completeness, correctness and overall detection quality were calculated with the help of the corresponding true positives, false positives and false negatives. The overall change

Table 2
Part of the developed Rules Set regarding the classification of the original data.

Domain	Class name	Features	Membership function	Threshold value (original)	Purpose
Unclassified	Changes to tiled roofs	Relative Area of sub objects MAD4+	Larger than	0.3–0.35	To classify new buildings with tiled roofs as indicated in MAD4
Real tiled roof	Buildings of 2003	Mean red 2003	Larger than	730–750	To identify buildings of 2003 that may have been incorrectly classified as changes
Real tiled roof with rectangular fit ≥0.6	Image object fusion with candidate condition for Target Objects, Rectangular fit≥ 0.8				To create more compact and rectangular objects
Real tiled roof	A set of loop sub-processes of region grown algorithm with Candidate condition: Rel. border to real tiled roof ≥0.3, candidate class: unclassified objects with Mean diff. of blue 2007 ≥150 to real tiled roof objects				To refine the borders of classified objects
Unclassified	Changes to bright roofs	Relative area of sub objects MAD4−	Larger than	0.3–0.35	To classify new buildings with bright roofs as indicated in MAD4
Real Changes to bright roofs I	Unclassified	Mean blue 2003	Larger than	410–450	To detect buildings of 2003 that were incorrectly classified as changes
Real changes to bright roofs	A set of loop sub-processes of region grown algorithm with candidate condition Rel. border to Changes to Bright Roofs I ≥0.3, Candidate class: unclassified objects with mean diff. of blue 2007≥−100 to real changes to bright roofs				To refine the borders of classified objects
Unclassified	Changes to dark roofs	Relative area of sub objects MAD3−	Larger than	0.5–0.6	To classify new buildings with dark roofs as indicated in MAD3
Changes to dark roofs	A loop process of region grown algorithm, Candidate objects: unclassified with Rel. border to changes to dark roofs ≥0.7				To refine the borders of classified objects

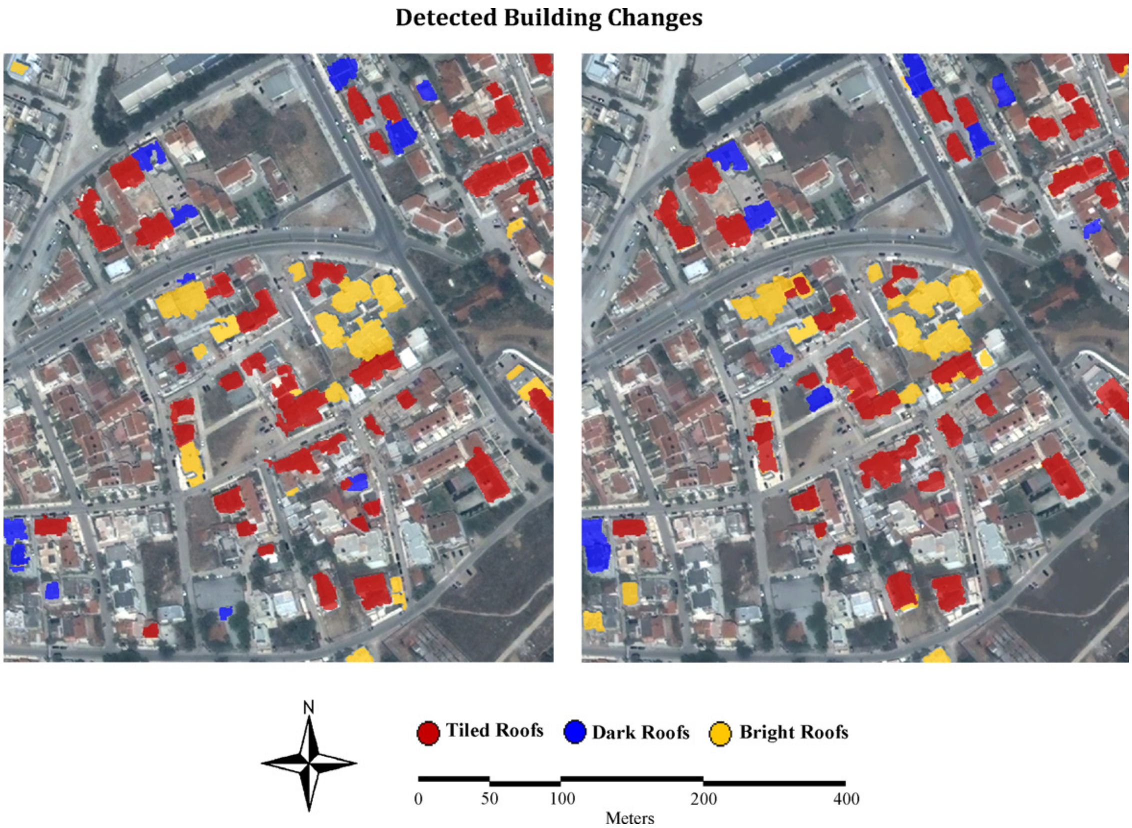

Fig. 7. Change detection results from the developed multilevel knowledge-based classification when the MAD components have been calculated: on the raw data (left) and the simplified data (right).

Fig. 8. Change detection results when the MAD components have been calculated on the simplified data. The purple pixels are the correctly detected changes (true positives), the yellow pixels are the false alarms (false positives: 4744 pixels) and the blue pixels are ones that did not detected (false negative: 13678 pixels).

Fig. 9. Change detection results when the MAD components have been calculated on the raw data. The purple pixels are the correctly detected changes (true positives), the yellow pixels are the false alarms (false positives: 5369 pixels) and the blue pixels are ones that did not detected (false negative: 16075 pixels).

Table 3
Quantitative performance evaluation.

Quantitative measures	Filtered dataset		Raw dataset	
	Object-based performance evaluation	Pixel-based performance evaluation	Object-based performance evaluation	Pixel-based performance evaluation
Completeness	95%	72%	62%	68%
Correctness	100%	88%	95%	86%
Quality	95%	66%	89%	61%

detection correctness of the developed methodology reached 100% with the object-based criteria and approximately 88% with the pixel-based ones. Regarding the completeness the algorithm scored relative high reaching 95% and 72%, respectively. In particular, only four (out of eighty) changed objects were not detected. All omissions were referring to cases of expansions or really small-sized buildings, with area smaller than 60 m^2 (165 pixels approximately). Moreover, the developed methodology managed to avoid the detection of any entirely false positive object and the only false alarms were pixels of the detected object boundaries. Regarding the overall change detection quality the developed methodology had a relative high performance reaching 95% for the object-based and 66% for the pixel-based criteria.

It is worth mentioning that the major difficulty for the delineation of the exact shape of the buildings was the fact that the images were acquired at off-nadir acquisition angle. The satellite images are generally acquired at off-nadir angles, because the temporal resolution is higher (<3 days) when the sensor is tilted to an off-nadir look angle. Specifically, the Quickbird images of 2003, 2007 and 2008 were acquired with off-nadir view angles 21.9°, 18.4° and 19.4°, respectively. The corresponding angles for Ikonos images of 2000 and 2006 were 20.8° and 21.4°. For this reason, not only the roofs, but also part of the building sides, were occluded making the detection of the correct geometric shape with a model-free approach quite difficult. These artifacts could be only eliminated by true ortho-photo generation methodologies. However, these processes are complicated to be implemented and yet under investigation. They also require stereo satellite images for the production of the digital surface model, increasing significantly the cost and the processing time of a multitemporal analysis.

We further evaluated the developed knowledge-based classification scheme by measuring its quantitative performance when the MAD components were calculated directly based on the raw data and not on the simplified images. In this case all the scoring rates were decreased indicating the importance and the efficiency of the morphological scale space simplification process. For the object-based performance evaluation the correctness decreased to 95% and the overall quality to 89%. In particular, six objects from the ground truth were not detected at all and three objects were incorrectly classified (false alarms).

The experimental results and the performed quantitative evaluation demonstrated the potential of the developed knowledge-based classification framework despite the difficulties towards the automation of such a procedure. In order to cope with the complexity of urban features, it was essential to combine spectral, geometric and topological information under an efficient object-oriented classification framework. Morphological scale space filtering was embedded in the processing scheme and improved the quality of the constructed object hierarchy. The simplified images provided meaningful objects that facilitated the classification procedure. A lower number of rules requires less time for tuning the system, a fact that affects not only the time of system implementation but also system transferability. Moreover, the performed evaluation underlined that most of the omitted pixels were parts of detected object boundaries mainly due to the approximately 20° off-nadir angle acquisition. This problem had also emerged during the ground truth production.

5. Conclusions and future work

An approach towards the land cover change detection, focusing mainly on buildings, was developed aiming at the (semi-) automated monitoring of the urban environment. Although, we did not use any ancillary data (like LIDAR data, existing geodatabases, etc.) the evaluation results demonstrated the potential of the proposed methodology. The elegantly simplified images from the morphological scale space filtering provided a more compact and reliable source, in order to generate image objects in various scales. Here elegantly refers to the behaviour of the filtering and mainly comments on its behaviour to preserve image edges and contours. The simplified data contributed to a fine segmentation and resulted to a more robust, simple and fast rule set structure. Moreover, the MAD transformation was able to detect the majority of urban changes with an automated way. An object-based approach for labelling the changes allowed the exploitation of spectral, shape and contextual information of urban features and produced an effective classification result. The incorporation of a model-based detection algorithm into the developed framework is currently under investigation in order to achieve a geometrically more accurate detection of terrain object shapes.

References

Alvarez, L., Lions, P.L., Morel, J.M., 1992. Image selective smoothing and edge detection by nonlinear diffusion. II. SIAM-JNA 29, 845–866.

Aplin, P., Smith, G., 2008. Advances in object-based image classification. International archives of the photogrammetry. Remote Sensing and Spatial Information Sciences 37 (Part B7), 725–728.

Baatz, M., Schape, A., 2000. Multiresolution segmentation an optimization approach for high quality multi-scale image segmentation. In: Strobl, J., et al. (Eds.), Angewandte Geographische Informationsverarbeitung XII. Wichmann, Heidelberg, pp. 12–23.

Baltsavias, E.O., 2004. Object extraction and revision by image analysis using existing geodata and knowledge: current status and steps towards operational systems. ISPRS, Journal of Photogrammetry & Remote Sensing 58, 129–151.

Benz, U., Hofmann, P., Willhauck, G., Lingenfelder, I., Heynen, M., 2004. Multiresolution, object-oriented fuzzy analysis of remote sensing data for GIS ready information. ISPRS Journal of Photogrammetry & Remote Sensing 58 (3–4), 239–258.

Bergen, K.M., Brown, D.G., Rutherford, J.F., Gustafson, E.J., 2005. Change detection with heterogeneous data using ecoregional stratification, statistical summaries and a land allocation algorithm. Remote Sensing of Environment 97, 434–446.

Blaschke, T., 2004. Towards a framework for change detection based on image objects. In: Erasmi, S., Cyffka, B., Kappas, M. (Eds.), Göttinger Geographische Abhandlungen, vol. 113, pp. 1–9.

Blaschke, T., 2010. Object based image analysis for remote sensing. ISPRS Journal of Photogrammetry and Remote Sensing 65 (1), 2–16.

Bouziani, M., Goita, K., He, D.C., 2010. Automatic change detection of buildings in urban environment from very high spatial resolution images using existing geodatabase and prior knowledge. ISPRS, Journal of Photogrammetry and Remote Sensing 65 (1), 143–153.

Canty, M.J., 2007. Image Analysis, Classification and Change Detection in Remote Sensing (With Algorithms for ENVI/IDL). Taylor & Francis, Boca Raton (USA), pp. 249–253.

Champion, N., Rottensteiner, F., Matikainen, L., Liang, X., Hyyppä, J., Olsen, B.P., 2009. A test of automatic building change detection approaches. In: Stilla, U., Rottensteiner, F., Paparoditis, N. (Eds.), CMRT09, vol. XXXVIII, part 3/W4. IAPRS, Paris.

Champion, N., Boldo, D., Pierrot-Deseilligny, M., Stamon, G., 2010. 2D building change detection from high resolution satellite imagery: a two-step hierarchical method based on 3D invariant primitives. Pattern Recognition Letters 31 (9), 1138–1147.

Donnay, J.P., Barnsley, M., Longley, P., 2001. Remote Sensing and Urban Analysis. Taylor & Francis, London, pp. 3–18.

Hall, O., Hay, G., 2003. A multi-scale object-specific approach to digital change detection. International Journal of Applied Earth Observation and Geoinformation 4 (4), 311–327.

Hay, G., Castilla, G., 2006. Object-based image analysis: strengths, weaknesses, opportunities and threats. International Archives of the Photogrammetry, Remote Sensing and Spatial Information Sciences 36 (Part 4/C42) (on CD-ROM).

Holland, D.A., Sanchez-Hernandez, C., Gladstone, C., 2008. Detecting changes to topographic features using high resolution imagery. International Archives of

Photogrammetry, Remote Sensing and Spatial Information Sciences, Beijing, China XXXVII (Part B4), 1153–1158.

Im, J., Jensen, J.R., 2005. A change detection model based on neighborhood correlation image analysis and decision tree classification. Remote Sensing of Environment 99, 326–340.

Jensen, R.J., 2005. Introductory Digital Image Processing: A Remote Sensing Perspective, 3rd ed. Pearson Education, USA, pp. 470, 478–480.

Jin, X., Davis, C.H., 2005. Automated building extraction from high-resolution satellite imagery in urban areas using structural, contextual, and spectral information. EURASIP, Journal on Applied Signal Processing 14, 2196–2206.

Karantzalos, K., Argialas, D., Paragios, N., 2007. Comparing Morphological Levelings constrained by different markers. In: Banon, G., et al. (Eds.), Proc. 8th Int. Symp. Mathematical Morphology, Mathematical Morphology and its Applications to Signal and Image Processing. , pp. 113–124.

Karantzalos, K., Paragios, N., 2009. Recognition-driven 2D competing priors towards automatic and accurate building detection. IEEE Transactions on Geoscience and Remote Sensing 47 (1), 133–144.

Lang, S., 2008. Object-based image analysis for remote sensing applications: modeling reality – dealing with complexity. In: Blaschke, T., et al. (Eds.), Object-Based Image Analysis – Spatial concepts for knowledge-Driven Remote Sensing Applications. Springer, New York, pp. 3–28.

Li, D., Haigang, S., Ping, X., 2003. Automatic change detection of geo-spatial data from imagery. Geo-Spatial Information Science 6 (3), 1–7.

Lizarazo, I., Barros, J., 2010. Fuzzy image segmentation for urban land cover classification. Photogrammetric Engineering & Remote Sensing 76 (2), 151–162.

Lu, D., Mausel, P., Brondizio, E., Moran, E., 2004. Change detection techniques. International Journal of Remote Sensing 25 (12), 2365–2407.

Matikainen, L., Hyyppä, J., Ahokas, E., Markelin, L., Kaartinen, H., 2010. Automatic detection of buildings and changes in buildings for updating of maps. Remote Sensing 2, 1217–1248.

Meyer, F., Maragos, P., 2000. Nonlinear scale-space representation with morphological levelings. Journal of Visual Communication and Image Representation 11 (2), 245–265.

Meyer, F., 2004. Image simplification filters for segmentation. International Journal of Mathematical Imaging and Vision 20 (1–2), 59–72.

Nielsen, A.A., 1994. Analysis of regularly and irregularly sampled spatial, multivariate and multi-temporal data, Ph.D. dissertation, IMM, Technical University of Denmark, Lyngby, pp. 75–99.

Nielsen, A.A., Conradsen, K., Simpson, J.J., 1998. Multivariate alteration detection (MAD) and MAF postprocessing in multispectral, bitemporal image data: new approaches to change detection studies. Remote Sensing of Environment 64, 1–19.

Niemeyer, I., Marpu, P.R., Nussbaum, S., 2007. Change detection using the object features. In: Proc. of the IEEE International Geoscience and Remote Sensing Symposium, IGARSS'07, Barcelona.

Nussbaum, S., Menz, G., 2008. Object-Based Image Analysis and Treaty Verification: New Approaches in Remote Sensing – Applied to Nuclear Facilities in Iran. Springer-Verlag, Berlin, pp. 85–139.

Ouma, Y., Josaphat, S., Tateishi, R., 2008. Multiscale remote sensing data segmentation and post-segmentation change detection based on logical modeling: theoretical exposition and experimental results for forestland cover change analysis. Computers & Geosciences 34 (7), 715–737.

Ozdemir, B., Aksoy, S., Eckert, S., Pesaresi, M., Ehrlich, D., 2010. Performance measures for object detection evaluation. Pattern Recognition Letters 31 (10), 1128–1137.

Radke, R.J., Andra, S., Al-Kofahi, O., Roysam, B., 2005. Image change detection algorithms: a systematic survey. IEEE Transactions on Image Processing 14 (3), 294–307.

Smith, G.M., Morton, R.D., 2010. Real world objects in GEOBIA through the exploitation of existing digital cartography and image segmentation. Photogrammetric Engineering & Remote Sensing 76 (2), 163–171.

Steinnocher, K., Kressler, F., 2006. Change Detection, Final Report, EuroSDR Project.

Sui, H., Zhou, Q., Gong, J., Ma, G., 2008. Processing of multi-temporal data and change detection. In: Li, Z.L, Chen, J., Baltsavias, E. (Eds.), Advances in Photogrammetry, Remote Sensing and Spatial Information Sciences: 2008 ISPRS Congress Book. Taylor & Francis, Nottingham, pp. 227–247.

Tzotsos, A., Karantzalos, K., Argialas, D. Object based image Analysis through scale space filtering. ISPRS Journal of Photogrammetry and Remote Sensing, in press.

Zhou, W., Huang, G., Troy, A., Cadenasso, M., 2009. Object-based land cover classification of shaded areas in high spatial resolution imagery of urban areas: a comparison study. Remote Sensing of Environment 113 (8), 1769–1777.